An Approach for Accidental Identification Victim Using Fingerprint and Iris Technology

Mohammed Mahmood Ali [1], Mohammed Luqman [2], Md. Sadeq Mohiuddin Ghori[3], Rabia Basri[4], Ateeq ur Rahman [5]
[1, 2] Department of CSE, MJCET, Student of Engineering, Osmania University, Telangana, India
[3, 4] Department of CSE, SWCET, Telangana, India
[5] Department of CSE, SCET, Telangana, India
Email: [1] mahmoodedu@gmail.com, [2] luq8055man@gmail.com, [3] sadeqghori531@gmail.com, [4] rabiabasri42@gmail.com, [5] mail_to_ateeq@yahoo.com
[1] Corresponding Author

Abstract—**Dynamically identifying of accidental victims on roads are the crucial challenges faced internationally by Traffic authorities, hospitals, and police personal. This paper proposes an advanced system for automating the identification of accident victims, utilizing fingerprint and iris biometrics to retrieve personal data from official databases such as Aadhaar, PAN, and voter ID. Rapid identification is critical in emergencies that assist in notifying to family members that aids to facilitate for immediate medical care, and at the same time streamline administrative response from health insurance and police officials. Traditional methods, however, are often slow and unreliable, particularly when victims' fingerprints or irises are damaged. To address these limitations, this system incorporates both fingerprint and iris recognition, along with a secondary identification method that enables data retrieval even when biometric data is compromised. In such cases, the system accepts alternative unique identifiers, including Aadhaar numbers, driver's license, passport IDs, or PAN IDs, to access the victim's information. The system leverages the Scale-Invariant Feature Transform (SIFT) algorithm to ensure high accuracy of 97.3%, overcoming the challenges of degraded fingerprints or other environmental impacts. By automating data retrieval and generating detailed reports, the system allows for the prompt notification of victims' families and reduces the workload on government and healthcare agencies. This approach not only improves the efficiency and accuracy of victim identification, but also ensures a more compassionate response, minimizing delays and distress for affected families. Consequently, this solution contributes significantly in enhancing the emergency response system by providing a reliable, multi-modal method for identifying accident victims under challenging circumstances.**

Keywords— Accidental victims, Fingerprint Matching, Iris biometric, PAN IDs, SIFT

I. INTRODUCTION

In emergency situations, particularly those involving accidents, rapid victim identification is crucial for providing timely medical care, notifying families, and ensuring effective coordination among emergency response teams. However, current victim identification methods are largely manual, which can be time-consuming and prone to errors [1]. When victims are unable to identify themselves and their documents are unavailable, delays in identification not only exacerbate the emotional distress for families but also increase the administrative burden on government, medical, and law enforcement agencies [2].

Recent advancements in biometric recognition had a great potential for improving the victim identification process. Biometric identifiers are extensively used namely fingerprints and iris patterns are unique to each individual and remain relatively stable over a lifetime, making them as reliable tools for identity verification purpose [3]. Fingerprints have long been a cornerstone of biometric systems due to their stability and widespread use in identification protocols [4] [25], while iris recognition is gaining attention for its precision and resistance to aging [5]. Nevertheless, single-modality biometric systems reveal limitations in real-world accident scenarios, where physical damage or environmental factors can compromise the integrity of biometric data, particularly fingerprints [6].

To address these challenges, a novel multi-modal identification system is proposed that combines fingerprint and iris recognition to enhance both accuracy and reliability. Multi-modal biometrics have proven to outperform single-modality systems, particularly in high-stakes applications like security and emergency response, by compensating for data loss or degradation [7], [8]. Moreover, in situations where biometric identification is not feasible, the system offers alternatives using unique identifiers such as Aadhaar numbers, driver's licenses, passport IDs, and PAN IDs [9]. By accessing authorized databases to retrieve personal information, this system ensures fast, accurate victim identification, filling critical gaps in current emergency response protocols.

The goal of this approach is to reduce response times, lighten the administrative load, and most importantly, provide a compassionate and efficient solution for promptly notifying victims' families. This paper explores the development and implementation of an advanced, automated identification framework that integrates multi-modal biometrics and database-driven data retrieval, streamlining emergency response and offering valuable support in critical situations.

Received: 8-1-2025
Revised: 30 -6-2026
Published: 30-6-2026

The structure of this paper is as follows: Section II, I illustrates the traditional fingerprint biometric methods as well as IRIS methods used to identify people. In Section III Illustrates the methods adopted in this research work for detection of accidental victims, while Section IV explores the result analysis and testing of the proposed approach using SIFT algorithm for Fingerprint and IRIS scan. In Section V, we present the conclusion of our research achievements and the performance metrics achieved. Finally, future enhancements are presented in Section VI..

II. Related Work

The literature survey reveals that significant advancements have been made in the field of biometric recognition, especially in fingerprint and iris technologies, to enhance the accuracy and robustness of automated identification systems. The key findings from the literature survey are as follows:

Methods involving dactylogram analysis have shown improved identification accuracy over manual identification. However, these approaches remain limited to Aadhar-based retrieval systems and require integration with Automated Details Retrieval Systems (ADRS) for broader use [10].

Techniques such as DeepIris that utilize deep learning models have demonstrated high accuracy and robustness to noise, occlusions, and environmental conditions. However, they face challenges due to high computational costs and the need for extensive training data [11].

Automated Details Retrieval System (ADRS) systems have proven efficient and precise for automated victim identification [24]. The primary drawback is their sensitivity to damaged fingerprints, which may limit their performance [12].

The advent of touchless 2D fingerprint and smartphone-based recognition systems has offered hygienic, user-friendly, and non-contact solutions. However, these systems are still sensitive to environmental factors, requiring further robustness improvements [13].

The Scale Invariant Feature Transform (SIFT) method provides strong matching accuracy and robustness against image rotation, scaling, and noise. However, its high memory consumption poses a limitation for real-time applications [14]. Overall, the findings emphasize the importance of developing robust, scalable, and multimodal biometric systems that integrate fingerprint and iris technologies.

III. Proposed Work

In this paper, we employed a desktop application using Python which takes input as fingerprint or Iris Scan Image and matches with various databases like Aadhar, Passport, Voter ID, PAN ID in order to generate the report of the victim.

The flow of this system architecture (Fig.1) is shown below:

Step 1: System receives fingerprint or iris scan data from the user

Step 2: Biometric data is pre-processed using different techniques.

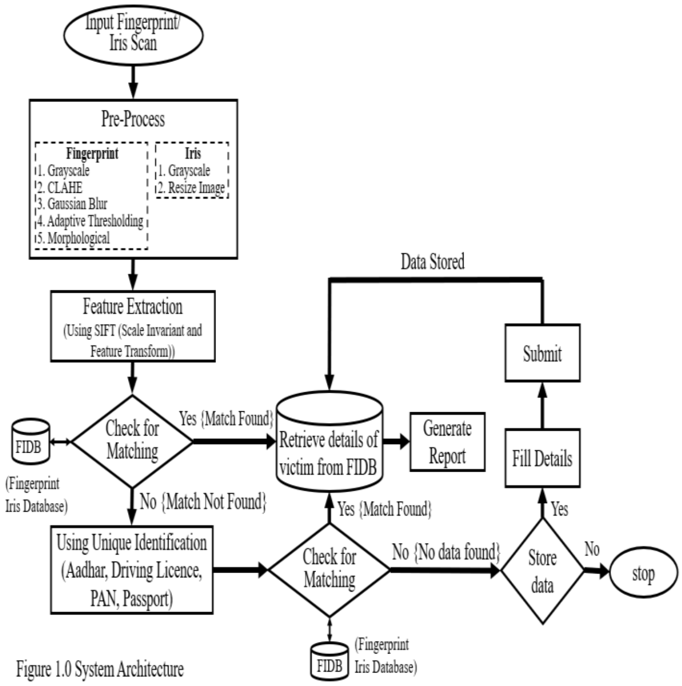

Fig. 1. System Architecture of Improvised ADRS using SIFT method

Step 3: Using SIFT (Scale-Invariant Feature Transform) to extract unique features from the processed biometric data

Step 4: System checks for matching in FIDB (Fingerprint/Iris Database). If match found go to step 5 else go to step 6.

Step 5: Retrieve details from FIDB and generate the report.

Step6: System takes input as unique IDs like Aadhaar, Driving License, or PAN/Passport and match with FIDB. If match found go to step 5 else go to step 7.

Step 7: System prompts whether to store data or not. If yes fill the details of the victim and submit else go to step 8.

Step 8: Stop

The data of FIDB database was taken from Kaggle. The FIDB contains Fingerprint Image, Iris Image, Name, Blood Group, Phone number, Address, Aadhar number, Ration ID, Voter ID and Passport Number.

Step I: The biometric image is first pre-processed using different techniques.

A. Fingerprint Pre-Process Steps:

Step 1: Conversion of Color image to Grayscale

i. Separate the Color Channels: For each pixel, get the red (R), green (G), and blue (B) values.

$$C(Color\ Image) = \begin{bmatrix} (255{,}0{,}0) & (0{,}255{,}0) & (0{,}0{,}255) \\ (128{,}128{,}0) & (128{,}0{,}18) & (0{,}128{,}128) \\ (255{,}255{,}255) & (0{,}0{,}0) & (50{,}100{,}150) \end{bmatrix}$$

ii. Apply the NTSC Formula (National Television Systems Committee) [15]: Compute the intensity I using the Equ. 1:

$$I=0.299\cdot R+0.587\cdot G+0.114\cdot B \quad (1)$$

These weights are based on the ITU-R BT.601 standard.

For example:

Apply NTSC formula to $C_{1,1}$:

$$G_{1,1} = 0.299 \cdot 255 + 0.587 \cdot 0 + 0.114 \cdot 0 = 76.245 \cong 76$$

Similarly calculate the gray value for each pixel.

iii. Assign Intensity to Pixel: Replace the original RGB values of the pixel with the calculated intensity I, making it a grayscale pixel [20].

$$G(Gray\ Image) = \begin{bmatrix} 76 & 150 & 29 \\ 114 & 61 & 94 \\ 255 & 0 & 92 \end{bmatrix}$$

Step 2: Enhancing Contrast using Contrast Limited Adaptive Histogram Equalization (CLAHE) derived values are depicted in Table I [16].

i. Divide the Image: The image is split into non-overlapping tiles of size $M \times N$ (e.g., 8x8).

ii. Apply Histogram Equalization in Each Tile: For each tile, histogram equalization is performed to spread out pixel intensities.

a. Calculate the probability $p(x)$ of each intensity level x in a tile.

b. Compute the cumulative distribution function (CDF) $C(x)$ for each intensity level using Equ. 2:

$$C(x) = \sum_{i=0}^{x} p(i) \quad (2)$$

c. Map the original intensity x to a new intensity x' using Equ. 3:

$$x'=(L-1)\times C(x) \quad (3)$$

where L is the total number of possible intensity levels (e.g., 256 for an 8-bit image).

iii. Clip the Histogram: After computing the histogram for each tile, it's limited to the clipLimit. Any values exceeding this limit are redistributed across all bins, preventing contrast over-amplification [21].

$$E(Equalized\ Matrix) = \begin{bmatrix} 113 & 226 & 56 \\ 198 & 85 & 170 \\ 255 & 28 & 141 \end{bmatrix}$$

TABLE I. CLAHE INTENSITY VALUES

Intensity Level (x)	**Frequ-ency**	**Probabil-ity (p(x))**	**C(x)**	**New intensity (x')**
0	1	1/9=0.111	0.111	255X0.111=28
29	1	1/9=0.111	0.111+0.111=0.222	255X0.222=56
61	1	1/9=0.111	0.222+0.111=0.333	255X0.333=85
76	1	1/9=0.111	0.333+0.111=0.444	255X0.444=113
92	1	1/9=0.111	0.444+0.111=0.555	255X0.555=141
94	1	1/9=0.111	0.555+0.111=0.666	255X0.666=170
114	1	1/9=0.111	0.666+0.111=0.777	255X0.777=198
150	1	1/9=0.111	0.777+0.111=0.888	255X0.888=226
255	1	1/9=0.111	0.888+0.111=1.000	255X1.000=255

Step 3: Apply Gaussian Blur To Reduce the noise [17].

i. Create the Gaussian Kernel: A kernel (a matrix of weights) is generated based on the below Gaussian function shown in Equ. 4:

$$G(x,y) = \frac{1}{2\pi\sigma^2} e^{-\frac{x^2+y^2}{2\sigma^2}} \quad (4)$$

where x and y are the pixel coordinates relative to the center of the kernel.

σ is the standard deviation, controlling the spread (or "width") of the Gaussian curve.

ii. Convolve the Image with the Kernel: For each pixel in the image, replace the pixel's intensity with the weighted sum of the surrounding pixels within the kernel.

iii. Each neighboring pixel's intensity is multiplied by its corresponding weight in the Gaussian kernel, and these values are summed to create the new intensity for the center pixel.

iv. For pixel P in the image with coordinates *(i,j)*, the new value P' is calculated as (Equ. 5):

$$P' = \sum_{x=-k}^{k} \sum_{y=-k}^{k} G(x,y).I(i+x,j+y) \quad (5)$$

where:

$G(x,y)$ is the Gaussian kernel value at position (x,y)

$I(i+x,j+y)$ is the intensity of the neighboring pixel at $(i+x,j+y)$

k is half the kernel size.

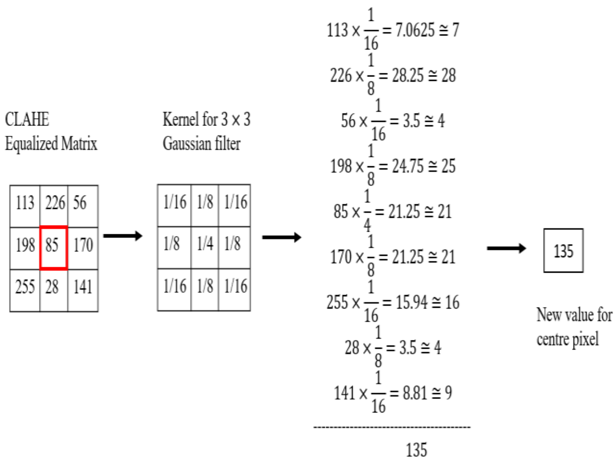

So similarly by applying Gaussian filter to each pixel we get the following output:

$$P' = \begin{bmatrix} 87 & 111 & 69 \\ 122 & 135 & 94 \\ 97 & 90 & 65 \end{bmatrix}$$

Step 4: Adaptive Thresholding is applied to ensure that fingerprint patterns are distinctly separated [18].

i. Define Local Neighborhood: For each pixel, a square neighborhood (or block) of size 11 x 11 is defined around it. The size is chosen based on the complexity of the image, with larger sizes giving smoother results.

For example: Consider 3 x 3 neighborhood for the below matrix:

$$\begin{bmatrix} 87 & 111 & 69 \\ 122 & \boxed{135} & 94 \\ 97 & 90 & 65 \end{bmatrix}$$

ii. Calculate Local Threshold: Within each neighborhood, calculate the mean pixel intensity. Then, subtract the constant to get the threshold for that specific pixel using Equ. 6.

$$\textit{Threshold=Mean of Block-C} \qquad (6)$$

$$M(Mean\ of\ Block) = \frac{87+111+69+122+135+94+97+90+65}{9}$$

$$= \frac{870}{9} \cong 97$$

where C is the constant to be subtracted.

Let C=3

$$Threshold = 97 - 3 = 94$$

iii. Apply Threshold: If the pixel's intensity is greater than or equal to this threshold, it is set to 0 (black); if it is less, it is set to 1 (white).

Since 135 > 94 so replace 135 by 0.

$$\begin{bmatrix} 87 & 111 & 69 \\ 122 & \boxed{0} & 94 \\ 97 & 90 & 65 \end{bmatrix}$$

Similarly apply this to each pixel we get the following result:

$$\mathrm{T} = \begin{bmatrix} 1 & 0 & 1 \\ 0 & 0 & 0 \\ 1 & 1 & 1 \end{bmatrix}$$

Step 5: Morphological Operations are applied to enhance the ridges in the fingerprint image, which improves the clarity of ridge structures and fills in gaps between them [19].

Dilation: The dilation step expands the white pixels in the binary image by placing the structuring element over each white region. This process fills in small black holes and connects nearby ridges.

Erosion: After dilation, the erosion step reduces the white regions back to their original size, but with the gaps filled and narrow connections retained. Erosion cleans up the expanded regions, maintaining the general shape of the ridges.

For an image T and a structuring element K, morphological closing is defined as shown in Equ. 7:

$$T \odot K = (T \oplus K) \ominus K \qquad (7)$$

where, $T \oplus K$ represents dilation of T by K.

$T \ominus K$ represents erosion of T by K.

$\odot$ indicates the closing operation.

$$\mathrm{T} = \begin{bmatrix} 1 & 0 & 1 \\ 0 & 0 & 0 \\ 1 & 1 & 1 \end{bmatrix} ;\ \mathrm{K} = \begin{bmatrix} 1 & 1 \\ 1 & 0 \end{bmatrix}$$

Dilation: Place the structuring element on every pixel of T such that if the origin matches with the pixel then replace that part of image with the structuring element as shown below:

Since $T_{1,1} = K_{1,1}$ so replace $T_{1,1}, T_{1,2}, T_{2,1}$ and $T_{2,2}$ with K

$$\mathrm{T} = \begin{bmatrix} \boxed{1 \quad 0} & 1 \\ \boxed{0 \quad 0} & 0 \\ 1 \quad 1 & 1 \end{bmatrix} ;\ \mathrm{K} = \begin{bmatrix} \boxed{1} & 1 \\ 1 & 0 \end{bmatrix}$$

origin

$$\mathrm{T'} = \begin{bmatrix} \boxed{1 \quad 1} & 0 \\ 1 \quad 0 & 1 \\ 1 \quad 1 & 1 \end{bmatrix}$$

Similarly performing for each pixel to obtain dilation matrix:

$$\mathrm{T} \oplus K = \begin{vmatrix} 1 & 1 & 1 & 1 \\ 1 & 1 & 1 & 1 \\ 1 & 1 & 1 & 1 \\ 1 & 1 & 1 & 0 \end{vmatrix}$$

Find closing by applying erosion on dilation matrix, this can be done finding structure matrix in dilation matrix as shown below and replacing the first element in each box with origin of structure element and replacing the other with zero.

$$K = \begin{bmatrix} 1 & 1 \\ 1 & 0 \end{bmatrix}$$

$$T \oplus K = \begin{vmatrix} 1 & 1 & 1 & 1 \\ 1 & 1 & 1 & 1 \\ 1 & 1 & 1 & 1 \\ 1 & 1 & 1 & 0 \end{vmatrix}$$

$$(T \oplus K) \ominus K = \begin{vmatrix} 0 & 0 & 0 & 0 \\ 0 & 0 & 0 & 0 \\ 0 & 0 & \boxed{1} & 0 \\ 0 & 0 & 0 & 0 \end{vmatrix}$$

$$T \odot K = \begin{vmatrix} 0 & 0 & 0 & 0 \\ 0 & 0 & 0 & 0 \\ 0 & 0 & 1 & 0 \\ 0 & 0 & 0 & 0 \end{vmatrix}$$

Fig.2. Fingerprint Pre-Process

B. *Iris Pre-process Steps:*

Step 1: Separate the Colour Channels: For each pixel, get the red (R), green (G), and blue (B) values.

Step 2: Apply the NTSC Formula (National Television Systems Committee) [15]: Compute the intensity I using the Equ. (1).

Step 3: Assign Intensity to Pixel: Replace the original RGB values of the pixel with the calculated intensity I, making it a grayscale pixel.

Step 4: Resize the image to 240x320 pixels.

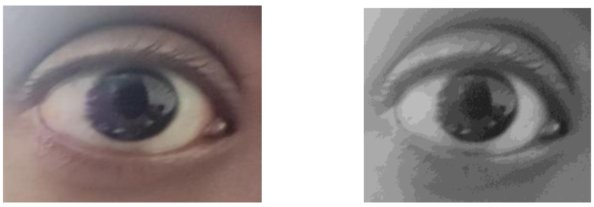

Fig.3. Iris Pre-Process

Step II: Now the features are extracted from pre-processed biometric image using Scale Invariant Feature Transform (SIFT) Algorithm [20],

Step 1: The first step involves constructing a scale-space to detect keypoints at different scales, making SIFT scale-invariant. This is done by repeatedly blurring the image with a Gaussian function and then subtracting consecutive blurred images to find distinctive features. The Difference of Gaussians (DoG) is used for this.

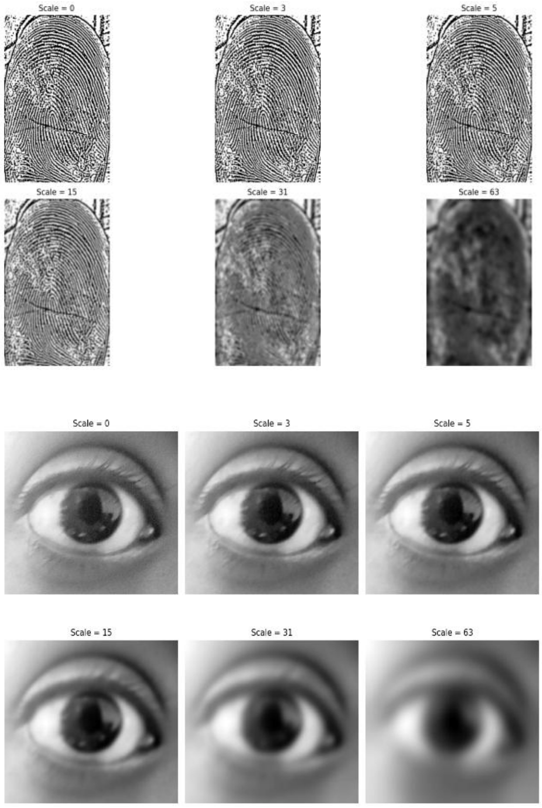

Fig.4. Gaussian Blur Images

i. Gaussian Blur (Equ. 8):

$$L(x, y, \sigma) = G(x, y, \sigma) * I(x, \quad (8)$$

where,

$L(x, y, \sigma)$ is the Gaussian Blurred image.

$G(x, y, \sigma)$is the Gaussian Function.

$I(x, y, \sigma)$ is the original image.

ii. DoG: The difference between images at adjacent scales is computed (Equ. 9):

$$D(x, y, \sigma) = L(x, y, \sigma) - L(x, y, k \quad (9)$$

where k is the constant scale factor.

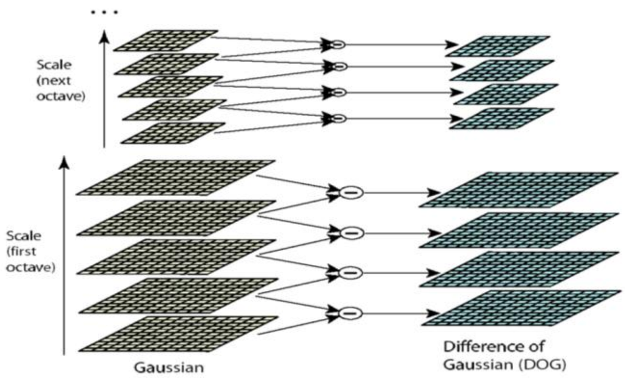

Fig.5. Difference of Gaussian

For example, the intensity of grayscale image is shown below:

$$I(x,y) = \begin{bmatrix} 76 & 150 & 29 \\ 114 & 61 & 94 \\ 255 & 0 & 92 \end{bmatrix}$$

Consider the coordinates of each intensity present in I as shown below:

$$\begin{bmatrix} (-1,1) & (1,0) & (1,1) \\ (-1,0) & (0,0) & (1,0) \\ (-1,-1) & (-1,0) & (1,-1) \end{bmatrix}$$

Now compute Gaussian for $\sigma = 3$ and $(x,y) = (-1,1)$ by substituting in Gaussian Function $G(x,y,\sigma) = \frac{1}{2\pi\sigma^2} e^{-\frac{x^2+y^2}{2\sigma^2}}$

$$G(-1,1,3) == \frac{1}{2\pi(3)^2} e^{-\frac{(-1)^2+(1)^2}{2(3)^2}} = 0.016$$

Similarly, by computing Gaussian for each intensity the following result is

$$G(x,y,3) = \begin{bmatrix} 0.016 & 0.017 & 0.016 \\ 0.017 & 0.018 & 0.017 \\ 0.016 & 0.017 & 0.016 \end{bmatrix}$$

Similarly compute Gaussian for $\sigma = 5$:

$$G(x,y,5) = \begin{bmatrix} 0.0061 & 0.0062 & 0.0061 \\ 0.0062 & 0.0063 & 0.0062 \\ 0.0061 & 0.0062 & 0.0061 \end{bmatrix}$$

$$L(x,y,3) = G(x,y,3) \times I(x,y,3)$$

Substitute $G(x,y,3)$ and $I(x,y)$ in the above equation:

$$L(x,y,3) = \begin{bmatrix} 0.016 & 0.017 & 0.016 \\ 0.017 & 0.018 & 0.017 \\ 0.016 & 0.017 & 0.016 \end{bmatrix} \times \begin{bmatrix} 76 & 150 & 29 \\ 114 & 61 & 94 \\ 255 & 0 & 92 \end{bmatrix}$$

$$L(x,y,3) = \begin{bmatrix} 7.23 & 3.44 & 3.53 \\ 7.68 & 3.65 & 3.75 \\ 7.23 & 3.45 & 3.53 \end{bmatrix}$$

Similarly compute $L(x,y,5)$:

$$L(x,y,5) = \begin{bmatrix} 2.73 & 1.21 & 1.32 \\ 2.77 & 1.31 & 1.34 \\ 2.73 & 1.21 & 1.32 \end{bmatrix}$$

Compute Difference of Gaussian:

$$D(x,y,4) = L(x,y,3) - L(x,y,5) = \begin{bmatrix} 4.5 & 2.23 & 2.21 \\ 4.91 & 2.34 & 2.41 \\ 4.5 & 2.24 & 2.21 \end{bmatrix}$$

Similarly calculate for $D(x,y,8)$

$$D(x,y,8) = L(x,y,7) - L(x,y,9) = \begin{bmatrix} 0.58 & 0.27 & 0.24 \\ 0.58 & 0.27 & 0.24 \\ 0.58 & 0.27 & 0.24 \end{bmatrix}$$

Maxima and minima of the difference of Gaussian images are detected by comparing a pixel (marked with X) to its 26 neighbours in 3x3 regions at the current and adjacent scales (marked with circles). So, these maxima and minima points are considered as potential keypoints. These potential keypoints (s_0) are not exact extremum points (Δs).

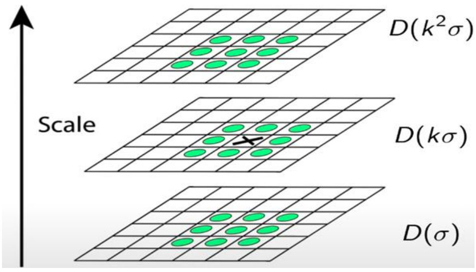

Fig.6. Detecting potential Keypoints

Step 2: Once potential keypoints are identified in the DoG images, they are refined by filtering out low-contrast points.

a. Taylor Expansion of scale space function (Equ. 10):

$$D(s_0 + \Delta s) = D(s_0) + \left(\frac{\partial D}{\partial s}\right)_{s_0} \Delta s + \frac{1}{2}\Delta s \left(\frac{\partial^2 D}{\partial s^2}\right)_{s_0} \Delta s \quad (10)$$

where $s_0 = (x_0, y_0, \sigma_0)$ and $\Delta s = (\delta_x, \delta_y, \delta_\sigma)$

b. The location of extremum, Δs (Equ. 11) is determined by taking the derivative of this function with respect to s and setting it to zero.

$$\Delta s = -\left(\left(\frac{\partial^2 D}{\partial s^2}\right)_{s_0}\right)^{-1} \left(\frac{\partial D}{\partial s}\right)_{s_0} \quad (11)$$

c. Next, reject low contrast points if $D(\Delta s)$ (Equ. 12) is smaller than threshold value which is 0.03 [20].

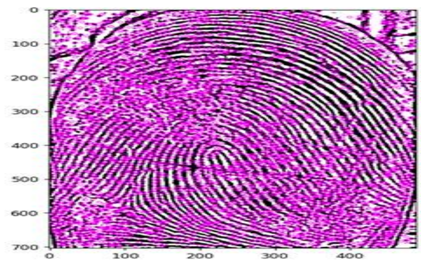

Fig.7. Keypoints in Fingerprint

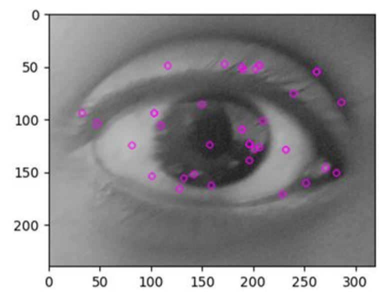

Fig.8. Keypoints in Iris

$$\frac{\partial D}{\partial s}=\begin{bmatrix}\frac{\partial D}{\partial x}\\ \frac{\partial D}{\partial y}\\ \frac{\partial D}{\partial \sigma}\end{bmatrix};\ \frac{\partial^2 D}{\partial s^2}=\begin{bmatrix}\frac{\partial^2 D}{\partial x^2} & 0 & 0\\ 0 & \frac{\partial^2 D}{\partial y^2} & 0\\ 0 & 0 & \frac{\partial^2 D}{\partial \sigma^2}\end{bmatrix}$$

TABLE II. CENTRE OF DIFFERENTIAL FORMULAE

Formulae	$(x,y)=(-1,0);$ $\sigma=\sigma_1=4;\sigma_2=8$
$\frac{\partial D}{\partial x}=\frac{D(x+1,y,\sigma)-D(x-1,y,\sigma)}{2}$	1.17
$\frac{\partial D}{\partial y}=\frac{D(x,y+1,\sigma)-D(x,y-1,\sigma)}{2}$	0
$\frac{\partial D}{\partial \sigma}=\frac{D(x,y,\sigma_1)-D(x,y,\sigma_2)}{\sigma_2-\sigma_1}$	1.1
$\frac{\partial^2 D}{\partial x^2}=D(x+1,y,\sigma)-2D(x,y,\sigma)+D(x-1,y,\sigma)$	−7.48
$\frac{\partial^2 D}{\partial y^2}=D(x,y+1,\sigma)-2D(x,y,\sigma)+D(x,y-1,\sigma)$	−0.82
$\frac{\partial D}{\partial \sigma}=\frac{D(x,y,\sigma_1)-D(x,y,\sigma_2)}{(\sigma_2-\sigma_1)^2}$	−0.27

$$\Delta s=-\left(\frac{\partial^2 D}{\partial s^2}\right)^{-1}\left(\frac{\partial D}{\partial s}\right) \qquad (12)$$

Substitute $\frac{\partial D}{\partial s}=\begin{bmatrix}1.17\\0\\1.1\end{bmatrix};\ \frac{\partial^2 D}{\partial s^2}=\begin{bmatrix}-7.48 & 0 & 0\\ 0 & -0.82 & 0\\ 0 & 0 & -0.27\end{bmatrix}$ into the above equation:

$$\Delta s=-\begin{bmatrix}-7.48 & 0 & 0\\ 0 & -0.82 & 0\\ 0 & 0 & -0.27\end{bmatrix}^{-1}\times\begin{bmatrix}1.17\\0\\1.1\end{bmatrix}$$

$$\Delta s=\begin{bmatrix}0.16\\ \boxed{0}\\ 4.07\end{bmatrix}$$

Each keypoint is assigned orientation based on the local gradient directions, making SIFT rotation-invariant. The various differential formulae values are shown in Table. II. The Compute Gradients, is calculated for each pixel around a keypoint, for gradient magnitude and orientation using Equ. 13 and Equ. 14:

Example: Keypoint is at (0,0):

$$L(x,y)=\begin{bmatrix}7.23 & 3.44 & 3.53\\ 7.68 & 3.65 & 3.75\\ 7.23 & 3.45 & 3.53\end{bmatrix}$$

$$m(x,y)=\sqrt{\left(L(x+1,y)-L(x-1,y)\right)^2+\left(L(x,y+1)-L(x,y-1)\right)^2} \qquad (13)$$

Substitute $(x,y)=(0,0)$

$$m(x,y)=\sqrt{\left(L(1,0)-L(-1,0)\right)^2+\left(L(0,\ 1)-L(0,\ -1)\right)^2}$$
$$=\sqrt{\left(L(1,0)-L(-1,0)\right)^2+\left(L(0,\ 1)-L(0,\ -1)\right)^2}$$
$$=\sqrt{(3.75-7.68)^2+(3.44-3.45)^2}=3.93$$

$$\theta(x,y)=\tan^{-1}\left(\frac{L(x,y+1)-L(x,y-1)}{L(x+1,y)-L(x-1,y)}\right) \text{-------} \qquad (14)$$

Substitute $(x,y)=(0,0)$:

$$\theta(0,0)=\tan^{-1}\left(\frac{L(0,1)-L(0,-1)}{L(1,0)-L(-1,0)}\right)=\tan^{-1}\left(\frac{3.44-3.45}{3.75-7.68}\right)=89^{\circ}$$

Orientation Histogram: An orientation histogram is created around each keypoint with 36 bins (covering 360°), weighted by the gradient magnitude and a Gaussian window. The peak in the histogram determines the main orientation of the keypoint.

Create histogram of gradient directions, within a region around the keypoint, at selected scale:

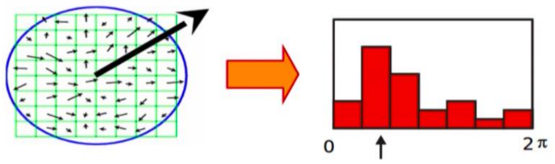

Fig.9. Histogram of Gradient Directions

Select the peak of histogram as direction of keypoint. Introduce additional key points at same location if another peak is within 80% of max peak of histogram with different direction.

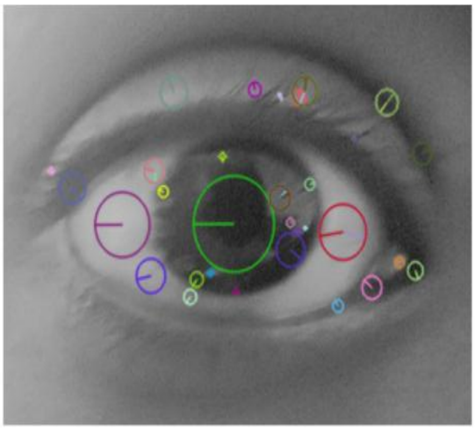

Fig.10. Features in Iris

Fig.11. Features in Fingerprint

Step III: Matching Descriptors using BFMatcher and L2 Norm :

A. BFMatcher: Brute-Force Matcher goes through every descriptor in the first set and matches it with every descriptor in the second set, finding the best match based on the smallest distance [21].

B. L2 Norm: The L2 norm, also known as the Euclidean distance [21], is used to measure the distance between two feature descriptors. Mathematically, for two descriptors d_1 and d_2 , the L2 norm (Euclidean distance) is given by (Equ. 15):

$$L2 = \sqrt{\sum_{i=1}^{n} (d_{1i} - d_{2i})^2} \qquad (15)$$

Step IV: Final Result:

Filter out the matches from step III based on the distance which are less than 50 [20].

If the number of good matches exceeds half of the total matches, return match otherwise, return not match.

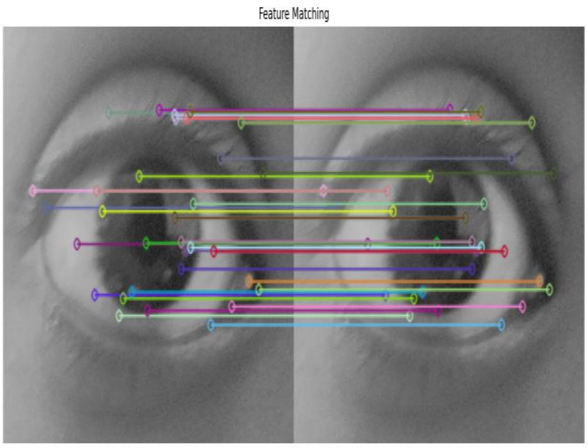

Fig.12. Iris Feature Matching

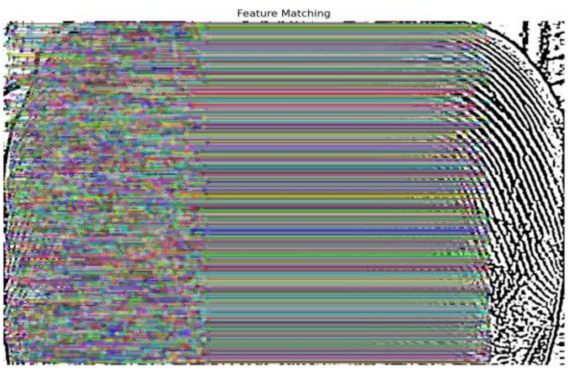

Fig.13. Fingerprint Feature Matching

IV. Results and Discussions

In Python, the implementation results using the SIFT Algorithm is performed. The report is generated as shown in Fig.14.

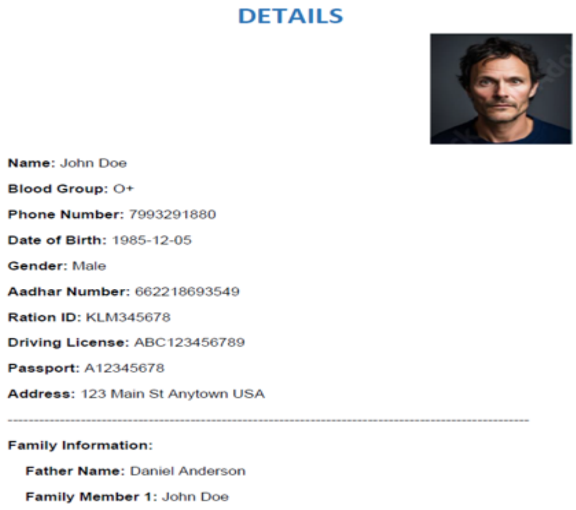

Fig. 14. Results retrieved by SIFT algorithm

The proposed system achieved an overall accuracy of 97.3% using the SIFT algorithm for fingerprint and iris recognition. This performance was compared with existing methods such as ORB (Oriented Fast and Rotated Brief), which achieved 65%, ORB with histogram equalization (HE) at 91.6%, and a simple CNN model that recorded 96.39% accuracy [12]. The results clearly indicate that the SIFT-based approach outperforms these existing methods, highlighting its effectiveness in extracting robust features for identification. Combining fingerprint and iris biometrics further enhanced accuracy, reducing false matches and improving the overall reliability of the system, especially in handling real-world data where fingerprints or iris scans may be partial or noisy.

The key findings demonstrate the significant improvement achieved by the proposed system. The integration of fingerprint and iris recognition not only enhances accuracy but also provides greater robustness compared to using individual modalities. While the ORB algorithm struggles with low-quality biometric inputs, and ORB with HE shows limited improvement, the SIFT algorithm's advanced feature extraction capabilities contribute to superior results. Additionally, the proposed system outperforms the simple CNN model by achieving higher accuracy, demonstrating the advantage of combining biometrics for accidental victim identification.

V. Conclusion And Future Scope

By integrating fingerprint and iris recognition technologies, the system addresses key challenges associated with conventional identification methods, particularly in cases where fingerprints are damaged or difficult to capture. Fingerprint-based identification methods often struggle in scenarios where the friction ridges are compromised due to injuries, burns, or wear. By incorporating iris recognition technology, which is less affected by physical damage, the proposed system ensures a more robust and reliable identification process. This dual-modality approach not only enhances the accuracy of identification but also provides a higher level of resilience against single-mode failures.

The use of the Scale-Invariant Feature Transform (SIFT) algorithm further reinforces the system's ability to handle varying conditions, including changes in illumination, orientation, and scale, while maintaining high accuracy. By retrieving data from multiple authoritative databases, the system improves its reliability, ensuring that accurate and up-to-date information is available for victim identification. This capability is particularly valuable in emergency situations where timely identification can expedite medical treatment and legal processes.

Overall, the integration of fingerprint and iris recognition technologies expedites the identification process, alleviates the distress of families by providing quick and reliable information, and reduces the operational burden on government and medical agencies tasked with managing accident victims. in large-scale scenarios.

The current system provides a solid foundation for accurate and efficient identification; however, future enhancements could focus on supporting real-time data updates, integrating cloud-based storage for improved accessibility, and incorporating machine learning algorithms to further optimize accuracy and processing speed. Additionally, developing a mobile application could enable on-the-spot identification for first responders in field operations. These enhancements would make the system more scalable, efficient, and adaptable to real-world scenarios.

REFERENCES

[1] National Institute of Standards and Technology (NIST), *Manual Identification Methods and Their Limitations*, Tech. Report, 2021.

[2] A. Mishra and P. Singh, "Challenges in Manual Victim Identification Processes," *Journal of Emergency Management*, vol. 8, no. 3, pp. 210–215, 2020.

[3] J. Daugman, "High Confidence Visual Recognition of Persons by a Test of Statistical Independence," *IEEE Transactions on Pattern Analysis and Machine Intelligence*, vol. 15, no. 11, pp. 1148–1161, 1993.

[4] K. Jain, A. Ross, and S. Prabhakar, "Fingerprint Matching Using Minutiae and Texture Features," *Proceedings of the International Conference on Image Processing*, vol. 2, pp. 282–285, 2001.

[5] A. Abhyankar and S. Schuckers, "A Novel Biorthogonal Wavelet Network System for Off-angle Iris Recognition," *Pattern Recognition*, vol. 43, no. 3, pp. 987–1007, 2010.

[6] M. A. U. Khan, "Challenges in Biometric Recognition Under Adverse Conditions," *IEEE Access*, vol. 5, pp. 12362–12375, 2017.

[7] A. Ross and A. K. Jain, "Information Fusion in Biometrics," *Pattern Recognition Letters*, vol. 24, no. 13, pp. 2115–2125, 2003.

[8] P. Drozdowski, C. Rathgeb, A. Uhl, and C. Busch, "Multimodal Biometrics: A Taxonomy and Survey," *Information Fusion*, vol. 57, pp. 3–35, 2020.

[9] Unique Identification Authority of India (UIDAI), Aadhaar and Its Applications in Emergency Identification, Technical Report, 2022.

[10] Ahmed Abdul Rafay, Dr. Sunil Vijay Kumar Gaddam, "Dactylogram to Identify Accident Victims a New Data Recovery Method", European Research, 2022.

[11] Shervin Minaee, Amirali Abdolrashidi, "DeepIris: Iris Recognition Using A Deep Learning Approach", ResearchGate, 2019.

[12] Dr Mohammed Mahmood Ali, "ADRS: Automated Details Retrieval System for victims of Incidents and Accidents using Fingerprint", International Journal of Computing and Digital Systems, 2022.

[13] Jannis Priesnitz, Christian Rathgeb, Nicolas Buchmann, Christoph Busch & Marian Margraf, "An overview of touchless 2D fingerprint recognition", Springer, 2021.

[14] Feng Guo, Jie Yang; Yilei Chen, Bao Yao, "Research on image detection and matching based on SIFT features", IEE International Conference, 2018.

[15] MathWorks Documentation, "How do I convert my RGB image to grayscale without using the Image Processing Toolbox?" *MathWorks*, Accessed: Aug. 2024. [Online].Available: https://www.mathworks.com/matlabcentral/answers/99136-how-do-i-convert-my-rgb-image-to-grayscale-without-using-the-image-processing-toolbox

[16] OpenCV Documentation, "CLAHE Implementation," *OpenCV*, Accessed: Aug. 2024. [Online].Available: https://docs.opencv.org/master/d5/daf/tutorial_py_histogram_equalization.html

[17] OpenCV Documentation, "Image Filtering: Gaussian Blur," *OpenCV*, Accessed: Aug. 2024. [Online]. Available: https://docs.opencv.org/4.x/d4/d13/tutorial_py_filtering.html

[18] OpenCV Documentation, "Adaptive Thresholding," *OpenCV*, Accessed: Aug. 2024. [Online]. Available: https://docs.opencv.org/4.x/d7/d4d/tutorial_py_thresholding.html

[19] OpenCV Documentation, "Morphological Transformations," *OpenCV*, Accessed: Aug. 2024. [Online]. Available: https://docs.opencv.org/4.x/d9/d61/tutorial_py_morphological_ops.html

[20] David G. Lowe Computer Science Department University of British Columbia Vancouver, B.C., J. Priesnitz, C. Rathgeb, N. Buchmann, and et al., "An overview of touchless 2d fingerprint recognition," Journal of Image Video Processing, vol. 8, 2021.

[21] OpenCV Documentation, "BFMatcher Class Reference," *OpenCV*, Accessed: Aug. 2024. [Online]. Available: https://docs.opencv.org/4.x/d3/da1/classcv_1_1BFMatcher.html

[22] D. Durga Bhavani, K. Rajeswari, and N. Srinivas Naik, "Big data analytics on aadhaar card dataset in hadoop ecosystem," in First International Conference on Artificial Intelligence and Cognitive Computing, R. S. Bapi, K. S. Rao, and M. V. N. K. Prasad, Eds. Singapore: Springer Singapore, 2019, pp. 459–466.

[23] T. Lillicrap, J. Hunt, A. Pritzel, N. Heess, T. Erez, Y. Tassa, D. Silver, and D. Wierstra, "Continuous control with deep reinforcement learning," 2015. [Online]. Available: https://doi.org/10.48550/arXiv.1509.02971

[24] K. Arvind, K. Mahesh, and K. S. Rishabh, "Identification of unclaimed dead bodies- a possible aadhar based solution," IP Inter national Journal of Forensic Medicine and Toxicological Sciences, vol. 3, pp. 74–76, 2018.

[25] N. Evans, "Handbook of biometric anti-spoofing: Presentation attack detection," Springer, vol. 1533, p. 519, 2019. [Online]. Available: https://www.springer.com/gp/book/9783319926261 digital.